INIS—mf——13756

SA9300029

KING SAUD UNIVERSITY
COLLEGE OF ENGINEERING
RESEARCH CENTER

931103

Final Research Report   No. EE-3/1406

Advanced Nuclear Fuel Production by Using Fission-Fusion Hybrid Reactor

b y
T.A. Al-Kusayer, S. Sahin and M. Abdul Raoof

ABSTRACT

At the college of Engineering, King Saud University, Kingdom of Saudi Arabia, a research project called AYMAN has been initiated to lay out the main structure of a prototypical experimental fusion and fusion-fission (hybrid) reactor blanket in cylindrical geometry. This geometry is consistent with most of the current fusion and hybrid reactor design concepts in respect of the neutronic considerations.

In this project the fusion chamber is simulated by a cavity with a diameter of approximately 1.6 m inside a cylindrical blanket. Fusion neutrons of 14 MeV are produced by a target movable along the axis of the cylinder. The moveable neutron source will allow one to simulate a line source for integral experiments, which is a result of the linear nature of the Boltzmann transport equation.

The calculations have shown that a blanket with 13 cm thick natural UO_2 fuel zone and 17 cm thick Li_2O zone would have a self-sustaining tritium breeding for the fusion driver. By an appropriate dispersion of the Li_2O zone inside the graphite reflector it became possible to decrease the neutron leakage out of the reflector by a factor of two to three in favour of (adding to) tritium breeding performance.

The studies have further shown that 1 GWe fission-fusion reactor can produce up to 957 kg/year, which is enough to fuel five light Water Reactors of comparable power. Fuel production can be increased by increasing the fission-fusion power or by improving the multiplication factor through controlling the neutron leakage to the minimum.

1. INTRODUCTION

Recently, a great number of scientific publications [1-3] have reported about fusion-fission (hybrid) reactor system studies. Only limited experimental efforts taken in respect of fusion neutronics have concentrated primarily either on studies of purely tritium breeding blankets [4-6] or on homogeneous fissionable blocks [7-8].

For the simulation of hybrid reactor neutronics, an experimental blanket should comprise of at least four (or five) main components namely the first wall (the neutron multiplier zone for a thorium blanket with suppressed fission), the fuel zone, the tritium breeding zone and the reflector. Integral experiments should cover at least the fission rate, the tritium breeding, the neutron multiplication through the fission process and through (n,2n) reactions in the fissionable materials and the neutron multiplier [9] at higher neutron energies.

Early Japanese experiments have evaluated the absolute fission rate distributions in hybrid blanket assemblies [10] which is an appreciable contribution in this field.

An experimental program for integral hybrid neutronic studies, called LOTUS, has been initiated in Switzerland [9]. The Swiss experimental facility went operational in 1984 [11]. Though the LOTUS blankets are being planned to comprise all the important components of a hybrid blanket, the limited size of the experimental cavity having internal dimensions 2.46, 3.6 and 3.00 meters in width, length and height, respectively, and a bulky structure of the Haefely neutron generator [12] (the fusion neutron source) have obliged the Swiss program to be restricted to experimental blankets in plane geometry. Detailed studies in relation with this program have demonstrated that the neutron spectrum in the plane geometry greatly differs from that of the neutron spectra in a prospective fusion-fission (hybrid) power plant. This is a direct consequency of the different left boundary conditions on these types of blankets [13-19]. Due to this drastic spectral shifting (on an experimental blanket in plane geometry) it seems to us that it is necessary to plan a new experimental

program of a hybrid blanket in a closed geometry in 4π (cylindrical or spherical) in order to conduct hybrid neutronic studies having reliable spectral consistency with that of a future hybrid power plant [20-23]. For this reason, in the Kingdom of Saudi Arabia, a new research project named AYMAN, has been initiated to evaluate the main outlines of experimental fusion (hybrid) blankets [24].

Another important handicap of the experimental assemblies in the LOTUS program, is the fact that they need three dimensionals neutron transport calculational models for a proper analysis and interpretation of the experiment, due to the lack of a clear symmetry of the experimental set up.

In the present work, the main components and the neutronic performance of some prospective hybrid blankets are evaluated which were briefly reported in the ref. [25].

Chapter 2 describes the basic structure of the blanket. In chapter 3 detailed neutronic analysis of the investigated blankets are presented, followed by chapter 4 with discussions and conclusions.

2. Description of the blanket

Within the framework of the AYMAN program, the 14-MeV-fusion-neutrons will be produced by a moveable target along the axis of a cylindrical hybrid blanket. Making use of the linear character of the Boltzmann Transport Equation [26], it is possible to simulate a line source with a moveable point source for integral measurements.

The source strength S (n/cm. sec) along the length L (cm) of the simulated line source by a steady movement (constant velocity) of the target during the irradiation is given by :

$$S = \frac{Q}{L} \qquad (1)$$

Q (n/sec) : Yield of the target (point of the target source).

A prospective AYMAN hybrid blanket in cylindrical geometry is shown in figures 1 and 2. It consists of mainly the following components:

a) The cylindrical first wall is SS-316 with a thickness of 1.3 cm, as that of the first wall of the TFTR in Princeton. The fusion plasma chamber will be simulated by a cylindrical cavity with a radius of 78.7 cm.

b) The fuel rods are made of natural -UO_2 (10 mm diameter) with a sintering density of 80% and are covered with an aluminium cladding (D_o = 12 mm, D_i = 10.4 mm), as shown in figure 3. In the fuel zone, they are arranged hexagonally with a volume fraction of 42% for air to simulate a gas cooled blanket, Figure 4.

Figure 5 shows the dimensions (in mm) of the space in between the fuel rods, which will be available for some measuring probes, such as foil activation, mini-fission chambers, etc.

c) To study the tritium breeding, Li_2O contained in aluminium cans has been adopted.

The total thickness of fuel zone + Li_2O zone has been taken to be 30 cm. The interface between these zones has been varied to obtain a self-sustaining blanket in respect of tritium breeding, discussed in detail in Chapter 3.

d) The neutron reflector is of graphite with a thickness of 30 cm.

The total blanket thickness after the first wall is 60 cm; and the total height of the cylindrical blanket considered is 250 cm inclusive of 25 cm graphite reflectors at the top and bottom.

The above described AYMAN hybrid blanket has a clear symmetry around the axis of the cylinder. Hence it allows one to analysis and interpreate the experiment properly by applying one and two dimensional neutron transport calculational model for a line and point neutron source, respectively, as a driven.

Table I shows the material composition in different zones of the investigated AYMAN hybrid blankets.

The optimization of the blanket in respect of fusile and fissile material breeding (leading to its final structure) is described in the following chapter.

3. Numerical Calculations

All transport theoritical calculations were performed in the S_8-P_3 approximation with the ANISN [27] code in cylindrical geometry, with a buckling correction for a height of 250 cm, using 100 neutron energy group data from DLC-2F [28] and DLC-24 [29] libraries.

Initially the interface between the fuel zone and the tritium breeding zone was varied in order to obtain a self-sustaining blanket in respect of tritium breeding. The calculations have shown that a blanket with 10 ranges of natural -UO_2 rods (13 cm fuel zone thickness) and a Li_2O zone of 17 cm thickness has a tritium breeding ratio higher than unity.

In this blanket the neutron leakage fraction is about 0.13 per incident neutron. An elegant way to reduce the neutron leakage out of a hybrid blanket is given by dispersing the strong neutron absorber (Li-6) inside the graphite reflector in the form of a sandwich structure. This increase the neutron absorption in favour of a higher tritium production and reduces the neutron leakage out of the blanket.

Table II shows the most significant neutronic data obtained from the investigated blanket configurations indicated at the bottom of the table.

As afore-mentioned, blanket B with 10 fuel rods represents a self-sustaining blanket in respect of tritium breeding ratio just above 1 - needed for the fusion driver.

Different blanket structures - each with 10 fuel rods - with a dispersion of Li_2O inside the graphite reflector by keeping the same total thicknesses of the Li_2O zone (17 cm) and that of the graphite zone (30 cm) have shown a decrease in the neutron leakage out of the blanket, as compared to the blanket type B.

Blanket D has the highest tritium breeding and the total breeding ratios. The neutron leakage is reduced by a factor of 2.18, as compared to the leakage in blanket B.

Whereas the blanket type E has the highest fissile breeding ratio and lowest neutron leakage fraction. The latter is reduced by a factor of 3, as compared to the blanket B. But, the tritium breeding in the blanket E is reduced, as compared to the blankets B and D. A thin Li_2O layer between the first wall and the fuel zone (blankets F and G) leads to higher tritium production in Li-7, but the overall neutronic performance decreases, compared to blanket B.

Under these considerations, the blanket D can be assigned as the optimium blanket among the investigated configuration in respect of the neutron economy.

Figure 6 shows the spatial variation of the fusile and fissile breeding, the fission density and the fission neutron production in the fuel and tritium breeding zones of the blanket type D. One can recognize easily that the Li-6(n,α)T reaction is higher in the neighbourhood of the graphite zones and is depressed towards the middle of the Li_2O zones which clearly demonstrates the advantage of a sandwich structure in respect of the tritium breeding.

Figure 7 depicts threshold detector responses in the blanket type D for a point neutron source strength of 1.5×10^{11} n/sec, or a line source strength of 10^9 (sec.cm).

The activities A_i for the Cu(n,p), Fe(n,p) and Cu(n,2n) threshold detectors have been calculated according to :

$$A_i = \Sigma_i \cdot \Phi (1 - e^{-\lambda_i T}) \qquad (2)$$

Σ_i : Macroscopic threshold reaction cross section for 1 gram of detector foil

λ_i : Decay constant of the isotope produced by activation

T   : Irradiation time (8 hours)

The activities for the $Th^{232}(n,f)$ and $U^{238}(n,f)$ threshold detectors represent the fission rate per gram of the corresponding fissionable material in a miniature fission chamber.

One can see in figure 7 that with a relatively modest neutron generator yield of 1.5×10^{11} n/sec, the detector activities are sufficiently high enough to conduct experiments which could lead to the determination of the fast neutron flux spectra through unfolding methods.

It was felt that it would be worthwhile to investigate the neutron spectrum in different regions of the blanket D.

Figure 8 shows the neutron spectrum in the first wall. Though the 14-MeV peak dominates, but there is an important contribution to the spectrum which stems from the fission neutrons and also from the reflected fusion neutrons. The latter is a direct consequence of the cylindrical geometry of the blanket. The ratio of the 14-MeV-peak to the second maximum below 1 MeV is about 4.

Figure 9 depicts the neutron spectrum in the middle of the fuel zone. This spectrum is softer than in the first wall. The ratio of the 14-MeV-peak to the second maximum below 1 MeV is decreased to a value around 2. We remember that this ratio in a comparable LOTUS blanket had been evaluated as approximately 8 (see figure 3 in ref. [18]). This demonstrates clearly that the neutron spectrum in a plane geometrical hybrid blanket differs greatly from that of a spectrum in a prospective hybrid power plant. Where the hybrid blanket has to cover the fusion plasma by a space angle nearly 4π.

Figure 10 shows the neutron spectrum in the first Li_2O zone adjacent to the fuel zone.

Figures 11 and 12 shows the neutron spectra in the second and third Li_2O zones of the blanket D respectively. As the thicknesses of these zones are only 4 cm each, the drop in the lower energy neutron

flux is less drastical as compared to that in the first Li_2O zone with a thickness of 9 cm.

For a better comprehension of the shift in the neutron spectrum it is useful to investigate the average neutron energy in the blanket, defined in this work as :

$$E^* = \frac{\int E \cdot \Phi(E) \cdot dE}{\int \Phi(E) dE} \qquad (3)$$

The average energies against the blanket thickness is plotted in figure 13. There is a continuous decrease in neutron energy by deeper penetration with some small ossilations by passing from the graphite zones into the Li_2O zones where the average neutron energy shows a small increase due to the strong neutron absorption at lower energies.

Table III shows the characteristics of the neutron spectra at the right boundaries of different zones of the blanket D with penetration of the neutrons in this blanket (excluding the thermal energy group in the DLC-2 library below 0.4 eV). It is interesting to note that the neutron fraction 1.1791 entering the first Li_2O zone will be depressed to 0.6797. Furthermore, the neutron fractions 0.5044 and 0.2388 entering the second and third Li_2O zones will be depressed to 0.2932 and 0.1149, respectively.

The left leakage fraction from the graphite zones are negligable, whereas other zones reveal certain left leakage fractions, not negligable as compared to the right leakage fractions in the respective zones.

Table IV depicts the fraction of neutron right leakage above certain selected energies, such as, >10 MeV, >1 MeV and >0.1 MeV. These values reflect a great deal of information about the neutron spectra by deeper penetration in the blanket.

4. Discussion

The present work has evaluated the neutronic performance of a prospective experimental fusion-fission hybrid blanket in cylindrical geometry, as a closed geometry blanket is needed to perform reliable experiments in the field of hybrid neutronics.

By moving a point neutron source along the axis of the cylindrical blanket with a constant velocity, it is possible to simulate a line source. This would allow one to perform experiments in a one-dimensional cylindrical geometry conditions which would greatly facilitate the interpretation of the experiments with numerical codes. Furthermore, this geometry will be compatible with the tandem mirror hybrid reactor design concept [3].

The calculations have shown that an experimental blanket with 10 ranges of fuel rods, making a 13 cm thick fuel zone and a 17 cm thick Li_2O zone would give a self-sustaining blanket in respect of tritium breeding.

The investigations have demonstrate that the breeding characteristics of a hybrid blanket can be improved by dispersing the Li_2O zone into the graphite reflector in form of a sandwich structure. This measure also reduces the neutron leakage out of the blanket.

Although foil activation measurements require a relatively strong neutron source, our calculations have shown that a modest neutron generator with an output of 1.5×10^{11} n/sec would make it possible to activate threshold detector to satisfactory levels.

Finally, it would be worthwhile to discuss whether such an experimental facility would have any prolific aspect.

Table II shows that the maximum plutonium production among the blankets with 10 fuel rods would be possible with the blanket type E (0.6 per incident fusion neutron).

-10-

By using a neutron generator with an output of 1.5×10^{11} n/sec and by an operational program of 100 hours/month - which is hardly to achieve within the frame work of an experimental program - the total plutonium production would yield into 154 μ gr/year which will be generated in dilluted form in a UO_2 mass of more than 5 tons. A commercially available rotating target generator with a neutron source strength of 3×10^{12} n/sec would lead to the production of .003 gm plutonium per year. Even this value represents a plutonium concentration of less than one a ppb in the natural uranium which can not be extracted by chemical methods.

Hence, one can conclude easily that the prospective AYMAN hybrid blankets will not have any prolific potential.

According to the results we have achieved in Table II, with 4.06676 multiplication factor, the Pu^{239} fuel production in the blanket of 1 GWe fission-fusion hybrid reactor can be estimated as following

1 fusion neutron $\rightarrow$ 17.6 MeV

Therefore, 1 fusion reaction will give

17.6 MeV x 1.6021×10^{-13} watt.sec/MeV = 2.8197×10^{-12} watt.sec.

Therefore, the fusion neutron produced per sec. in 1 GWe reactor

is :

$$\frac{10^9}{2.8197 \times 10^{-12}} = 3.5465 \times 10^{20} \text{ fusion/sec.}$$

The number of Pu atoms produced per sec
= .43106 x 3.5465×10^{20} = 1.528×10^{20} Pu/sec

But we know that $N = \dfrac{Avo. \times M}{A}$

Therefore $M = \dfrac{N.A}{Avo} = \dfrac{1.528 \times 10^{20} \times 239}{6.023 \times 10^{23}} = 6.0633 \times 10^{-2}$ gm Pu/sec

Therefore, Pu production/year
= 6.0633×10^{-2} x 3.1557×10^{7} sec/year x 50 % (load factor)
= 9.5670×10^{5} gm = 956.70 kg/year.

To estimate the number of LWRs that can be fueled by utilizing the above new fuel, assuming 1000 MWe power of each reactor;

1 fission neutron → 200 MeV

Therefore, fission reaction produced by 1 Pu atom fuel,
200 MeV x 1.602 x 10^{-13} watt.sec/MeV = 3.2042 x 10^{-11} watt. sec.

Therefore, Pu inventory needed for every 1000 MWe fission reactor, can be calculated as

$$\frac{3 \times 10^9 \text{ watt x 3.1557 x } 10^7 \text{ sec/year x 60\% (load factor)}}{3.2042 \times 10^{-11} \text{ watt.sec/Pu}}$$

= 1.7728 x 10^{27} Pu atoms.

The total Pu fuel inventory needed to run one reactor can be calculated as

$$\frac{1.7728 \times 10^{27} \times 239}{6.023 \times 10^{23}} = 7.0345 \times 10^5 \text{ gm} = 703.45 \text{ kg fuel}$$

But for continuous operation of LWRs, the conversion factor of the reactor should be considered, therefore the continuous fuel consumption can be calculated as following

703.45 kg x (1-r) = 703.45 x .3 = 211.04 Kg

This means, one fission-fusion hybrid reactor (with comperable neutronic performance) can supply up to five light water reactors.

REFERENCES

1. Proceedings of US-USSR Symposium on Fusion-Fission Reactor, ILL-Report, CONF-760733 (July 13-16, 1976).

2. Youssef, M.Z., R.W. Conn : A survey of fusion-fission system designs and nuclear analysis, University of Wisconsin, UWFLM-308 (June 1979).

3. Lee, J.D., et al. : Feasibility study of a fission-supressed Tandem-mirror hybrid reactor, LLNL, UCID-19327 (April 1982).

4. Bachmann, H., et al. : Neutorn spectra and tritium production measurements in a lithium sphere to check fusion reactor blanket calculations, Nuclear Science and Engineering, Vol. 67, p. 74 (1978).

5. Kuijpers, L. : Experimental model studies for a fusion reactor blanket, Kernforschungsanlage Julich-Nr. 1356, Ph.D. Thesis (Nov. 1976).

6. Herzing, R. : Erprobung neutronenphysikalischer Rechenverfahren an Lithiumblanketmodellen für, einen Fusionsreaktor, Kernforschungsanlage Julich-Nr. 1357, Ph.D. Thesis (Dec. 1976).

7. Weale, J.W., et al. : Measurement of the reaction rate distribution produced by a source of 14 MeV neutrons at the center of a uranium metal pile, Journal of Nuclear Energy, Vol. 14, p. 91 (1961).

8. Shieff, H.E.J., et al. : Measurement of the reaction rate distributions produced in a large thorium cylinder by a central source of D-T neutrons, AWRE-Report NO. 0 20/77 Aldermaston, Berkshire, UK (July 1977).

9. Şahin, S., et al. : Basis structure of the fusion-fission (hybrid) reactor experimental research project in Laboratoire de genie atomique de l'EPFL, Atomkernenergie/Kerntechnik, Vol. 36, p. 33 (1980).

10. Maekawa, H., J. Seki : Absolute fission rate distributions in lithium and hybrid fusion blanket assemblies, (I) Experimental method and results, J. Nucl. Sc. Technol., Vol. 14, p. 97 (1977); (II) Analysis and Evaluation, J. Nucl. Sci. Technol., Vol. 14, p. 210 (1977).

11. Rapport d'activite 1984, Department of Physic, Swiss Federale Institute of Technology in Lausanne (1984).

12. Schmidt, K.A., G. Reinhold : The Haefely-GFK Fast Neutron Generator, Int. J. Radiation Oncology Biol Phys., Vol. 3, p. 373, Pergamon Press (1977).

13. Şahin, S., Calinon R., G.N. Woodruff : A Neutronic Analysis of Lanthanides as Neutron Multipliers for Hybrid and Fusion Blankets, Transactions of the American Nuclear Society, Vol. 35, p. 132 (Nov. 1980).

14. Şahin, S. : Investigation of lanthanides as neutron multipliers for hybrid and fusion reactor blankets, Nuclear Technology/Fusion, Vol. 40, p. 224, (1982).

15. Şahin, S. : A neutron physics analysis for the experimental facility LOTUS, Atomkernenergie/Kerntechnik, Vol. 41, p. 95 (1982).

16. Şahin, S., A. Kumar : Neutronic performance of some hybrid blankets with conventional and actinide-waste fuel, Transactions of the American Nuclear Society, Vol. 43, p. 207 (1982).

17. Kumar, A. S., S. Şahin : Investigation of neutronics of some (D,T)-driven experimental thorium hybrid blankets with actinide multipliers, Journal of Fusion Energy, Vol. 3, p. 185 (1983).

18. Şahin, S., A. Kumar : Neutronics analysis of (D,T)-driven experimental hybrid blankets, Fusion Technology, Vol. 6, p. 97, (1984).

-14-

19. Kumar, A., S. Şahin : (D-D)-driven experimental hybrid blankets and their neutronic analysis, Fusion Technology, Vol. 6, p. 225 (1984).

20. Şahin, S., T. A. Al-Kusayer : Advanced fusion fuel driven AYMAN hybrid blankets, 6th Miami International Conference on Alternative Energy Sources, Proceedings of condensed papers, p. 161, 12-14 Dec. 1983, Miami Beach, Florida.

21. Al-Kusayer, T. A., S. Şahin, S. Khan : (D,T) driven thorium hybrid blankets, 6th Miami International Conference on Alternative Energy Sources, Proceedings of condensed papers, p. 344, 12-14 Dec. 1983, Miami Beach, Florida.

22. Şahin, S., T. A. Al-Kusayer : Nuclear Waste Actinides as Fissile Fuel in hybrid blankets, 6th Miami International Conference on Alternative Energy Sources, Proceedings of condensed papers, pp. 350, 12-14 Dec. 1983, Miami Beach, Florida.

23. Al-Kusayer, T. A., S, Şahin : Natural Uranium Hybrid blankets for AYMAN project, 6th Miami International Conference on Alternative Energy Sources, Proceedings of condensed papers, p. 384, 12-14 Dec. 1983, Miami Beach, Florida.

24. Al-Kusayer, T. A., S. Şahin, M. Abdul Raoof : Advanced nuclear fuel production by using fission-fusion (hybrid) reactor, Project NO.16/404, Research Center, College of Engineering, King Saud University, Riyadh (1984).

25. Şahin, S., T. A. Al-Kusayer, M. Al-Semair, M. Abdul Raoof : Neutronic Investigations of experimental AYMAN hybrid blankets, Trans. Am. Nucl. Soc., Vol. 47, p. 151 (1984).

26. Weinberg, A. M., E. P. Wigner : The Physical Theory of Nuclear Chain Reactors, The University of Chicago Press (1959).

27. Engle, W. W. Jr. : ANISN, A One-Dimensional Discrete Ordinates
    Transport Code with Anisotropic Scattering, K-1693, Oak Ridge
    Gaseous Diffusion Plant (1970).

28. DLF-2F : 100-Group Neutron Cross-section Data Based on ENDF/B,
    RSIC-ORNL, Oak Ridge National Laboratory (1975).

29. SINEX, DLC-24 : 100-Group Neutron Reaction Cross-section Data
    Generated by SUPERTOG from ENDF/B, RSIC-ORNL, Oak Ridge National
    Laboratory (1973).

Table I. Material composition of the AYMAN Hybrid Blankets.

Zone	Material	Nuclide	Nuclei Density ($^*10^{30}$/m^3)
First Wall	SS-316	Si	1.7108E-3
		Cr	1.6627E-2
		Mn	1.7548E-3
		Fe	5.7651E-2
		Ni	8.1863E-3
		Mo	1.0022E-3
Fuel	natural -UO$_2$	O	1.79828E-2
		Al	8.70727E-3
		U-235	6.29401E-5
		U-238	8.92850E-3
Tritium breeding	Li$_2$O	Li-6	4.920E-3
		Li-7	6.068E-2
		O	3.280E-2
		Al	3.014E-3
Reflector	C	C	1.1284E-1

Table II. Neutronic performance of (n,T) driven hybrid blankets within the framework of AYMAN experimental program (per incident 14 MeV neutron).

Blanket type*	A	B	C	D	E	F	G
T_6	0.93837	0.89729	0.69702	0.94711	0.78201	0.84847	0.86052
T_7	0.24184	0.12575	0.053647	0.10497	0.049662	0.16908	0.1706
T	1.18021	1.02304	0.75066	1.05208	0.83167	1.01755	1.03113
$U^{235}(n,f)$	0.00627	0.01799	0.03052	0.018788	0.026191	0.015282	0.015185
$(n,f)_{total}$	0.09127	0.19099	0.25962	0.19202	0.2014	0.144	0.14387
$U^{238}(n,\gamma)$	0.136	0.40041	0.70692	0.43106	0.60451	0.36891	0.36516
Fusile+fissile breeding	1.31621	1.42345	1.45758	1.48314	1.43618	1.38646	1.39629
$U^{238}(n,2n)$	0.050386	0.094048	0.11873	0.094081	0.0945	0.074937	0.074934
Leakage	0.091456	0.13226	0.18198	0.060887	0.043552	0.076314	0.069059
M**	2.6245	4.029	4.947	4.06676	4.1443	3.347	3.3494
k_{eff}	0.23579	0.37837	0.4437	0.37961	0.3885	0.31182	0.311662

*   Structure of the blankets

A : 1.3 cm SS + 5 cm fuel (4 ranges) + 25 cm Li_2O + 30 cm C

B : 1.3 cm SS + 13 cm fuel (10 ranges) + 17 cm Li_2O + 30 cm C

C : 1.3 cm SS + 21 cm fuel (16 ranges) + 9 cm Li_2O + 30 cm C

D : 1.3 cm SS + 13 cm fuel + 9 cm Li_2O + 6 cm C + 4 cm Li_2O + 6 cm C + 4 cm Li_2O + 18 cm C

E : 1.3 cm SS + 13 cm fuel + 6 cm C + 5 cm Li_2O + 6 cm C + 6 cm Li_2O + 6 cm C + 6 cm Li_2O + 12 cm C

F : 1.3 cm SS + 3 cm Li_2O + 13 cm fuel + 10 cm Li_2O + 8 cm C + 4 cm Li_2O + 22 cm C

G : 1.3 cm SS + 3 cm Li_2O + 13 cm fuel + 11 cm Li_2O + 10 cm C + 3 cm Li_2O + 20 cm C.

** $M = \dfrac{\text{Fission energy release + neutron heat release in Lithium}}{14 \text{ MeV}} + 1$

Table III. Neutron spectrum characteristics in different zones of the blanket D.

Zone	Material	Lr(+)	Er(+)	Lr(-)	Er(-)
1	SS-316	1.0620	10.156E+6	0.0632	1.165E+6
2	natural - UO_2	1.1791	4.234E+6	0.0964	0.906E+6
3	Li_2O	0.6797	3.098E+6	0.1526	0.015E+6
4	C	0.5044	2.225E+6	0.00	-
5	Li_2O	0.2932	2.627E+6	0.0446	0.011E+6
6	C	0.2388	1.748E+6	0.00	-
7	Li_2O	0.1149	2.482E+6	0.0309	0.007E+6
8	C	0.0441	1.223E+6	0.00	-

Lr(+) : Fraction of the forward oriented neutrons at the right boundary.

Er(+) : Average energy of the forward oriented neutrons at the right boundary in eV.

Lr(-) : Fraction of the backward oriented neutrons at the right boundary.

Er(-) : Average energy of the backward oriented neutron at the right boundary in eV.

Table IV. Fractions of the forward oriented neutrons in different zones
of the blanket D.

Zone	Lr > 10 MeV	Lr > 2 MeV	Lr > 1 MeV	Lr > 0.1 MeV
1	0.7445	0.7573	0.8311	1.00
2	0.3035	0.4048	0.5100	1.0144
3	0.1265	0.1827	0.2209	0.4782
4	0.0649	0.1033	0.1302	0.1989
5	0.0440	0.0725	0.0889	0.1518
6	0.0228	0.0413	0.0525	0.0722
7	0.0153	0.0287	0.0355	0.0563
8	0.0022	0.0063	0.0087	0.0129
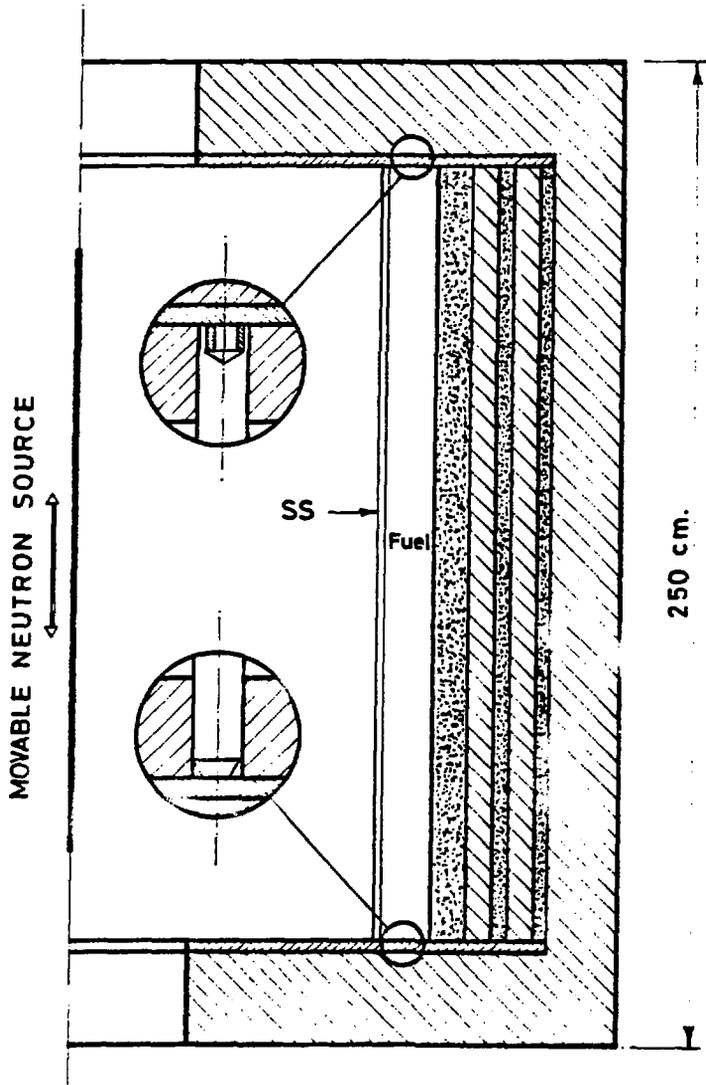
Figure 1. Basic structure of a AYMAN hybrid blanket
          (Blanket type D in table II)

          Mass of natural - UO_2 : 5.1 tons
          Mass of Li_2O : 1.48 tons
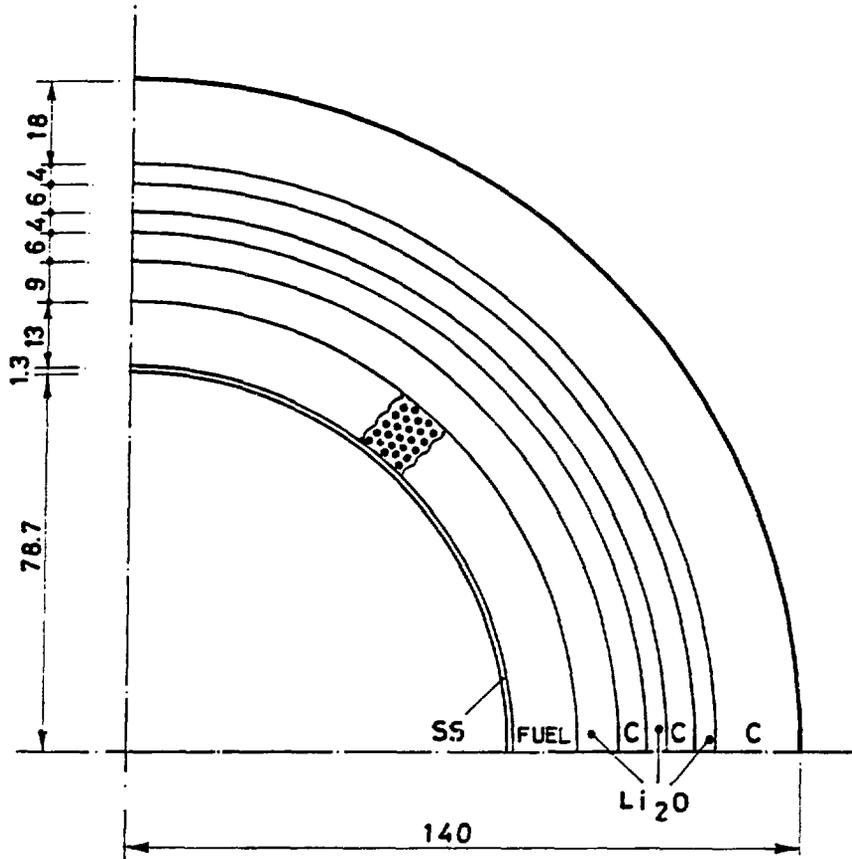
Figure 2. Cross sectional view of a AYMAN hybrid blanket, dimensions in cm. (Blanket type D in table II).
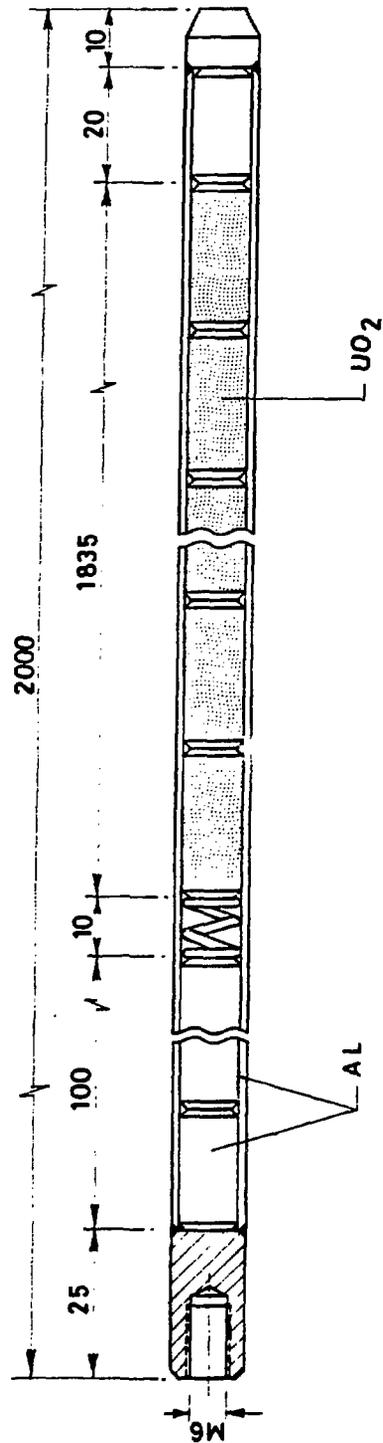
Figure 5. The dimensions (in mm) of a typical fuel rod in a prospective AYMAN hybrid blanket.
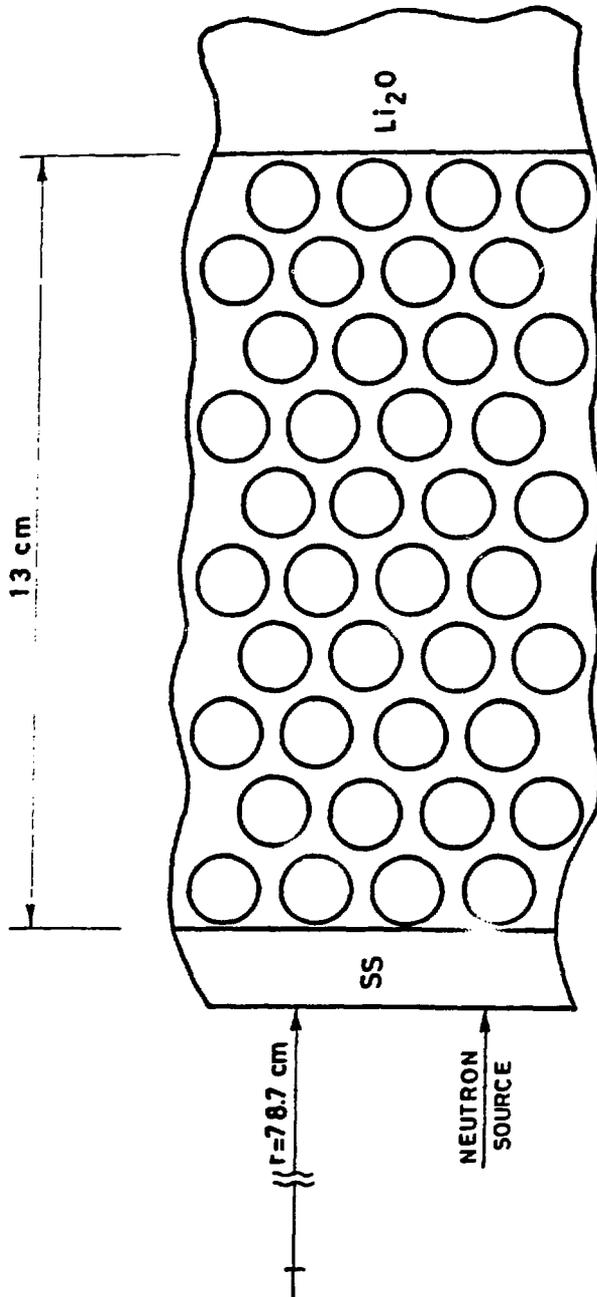
Figure 4. The arrangement of the fuel rods in the fuel zone of an AYMAN hybrid blanket.
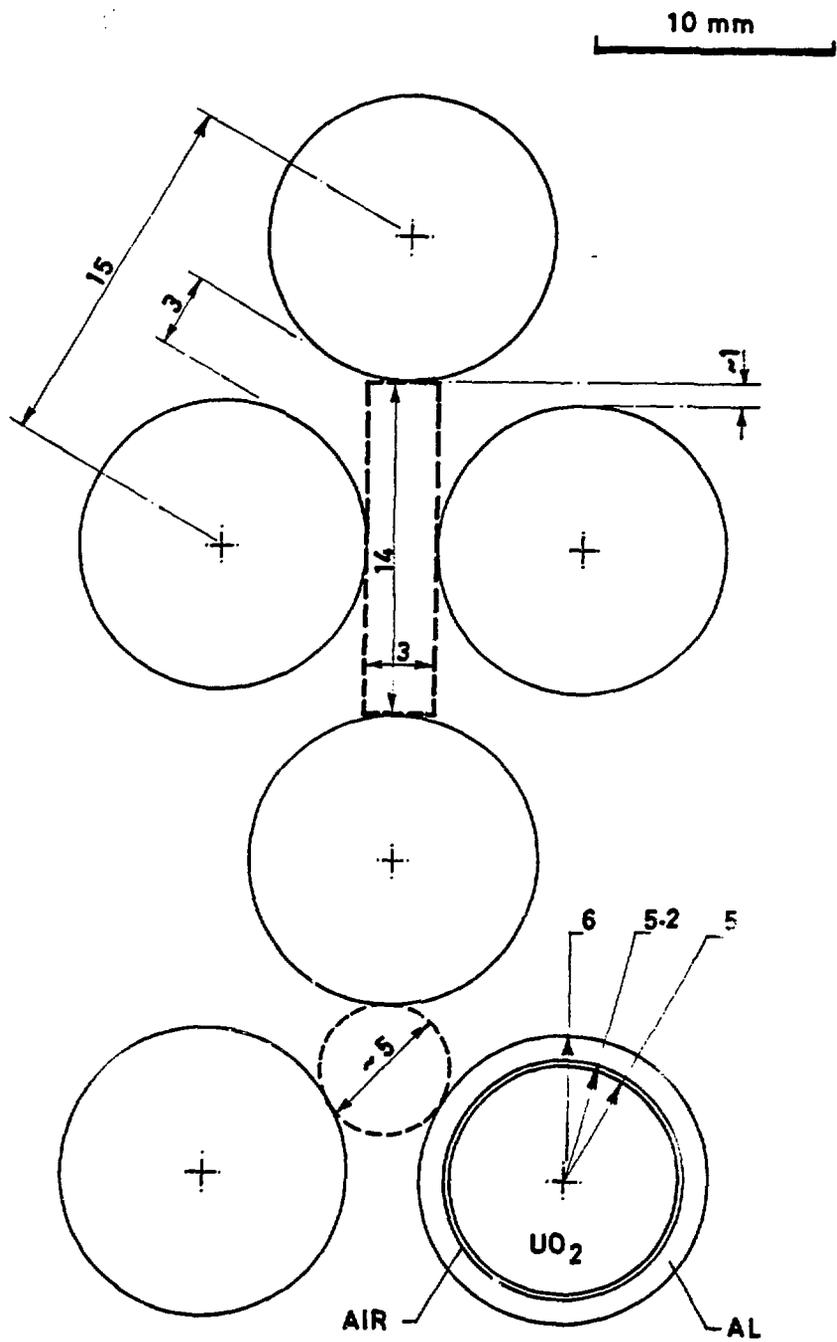
Figure 5.   The pitch dimensions (in mm) in the fuel zone of an AYMAN hybrid
blanket.

Figure 6. The fusile and fissile breeding, fission and neutron production
densities in the blanket type D
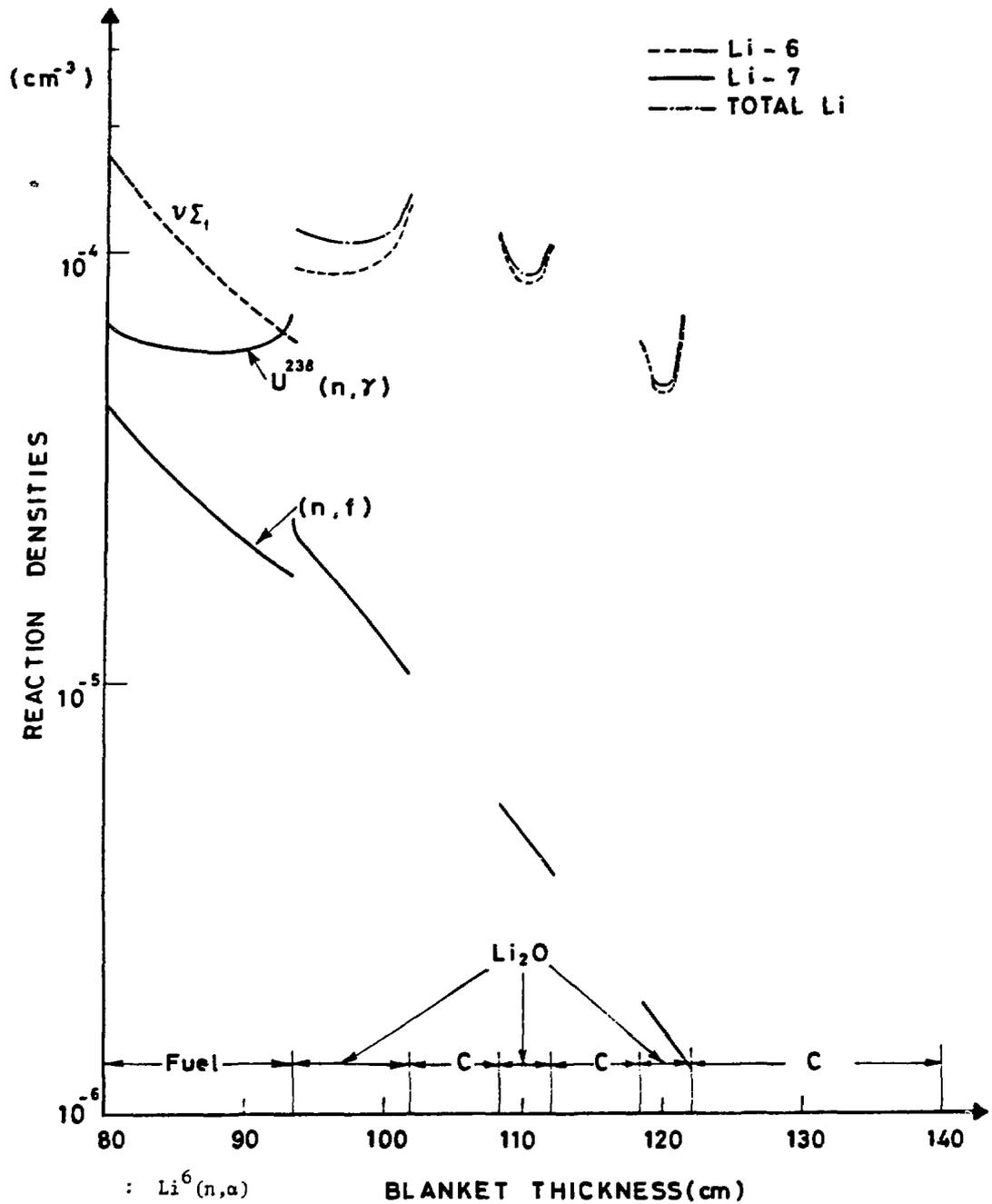
T_6 : $Li^6(n,\alpha)$

T_7 : $Li^7(n,n',\alpha)T$

$T = T_6 + T_7$: fusile breeding

$U^{238}(n,\gamma)$: fissile breeding

(n,f) : $\int \Sigma_f \phi dE$: fission density (fission power generation
                        profile)

$\nu\Sigma_f$ $\int \nu\Sigma_f \phi dE$: fission neutron generation.
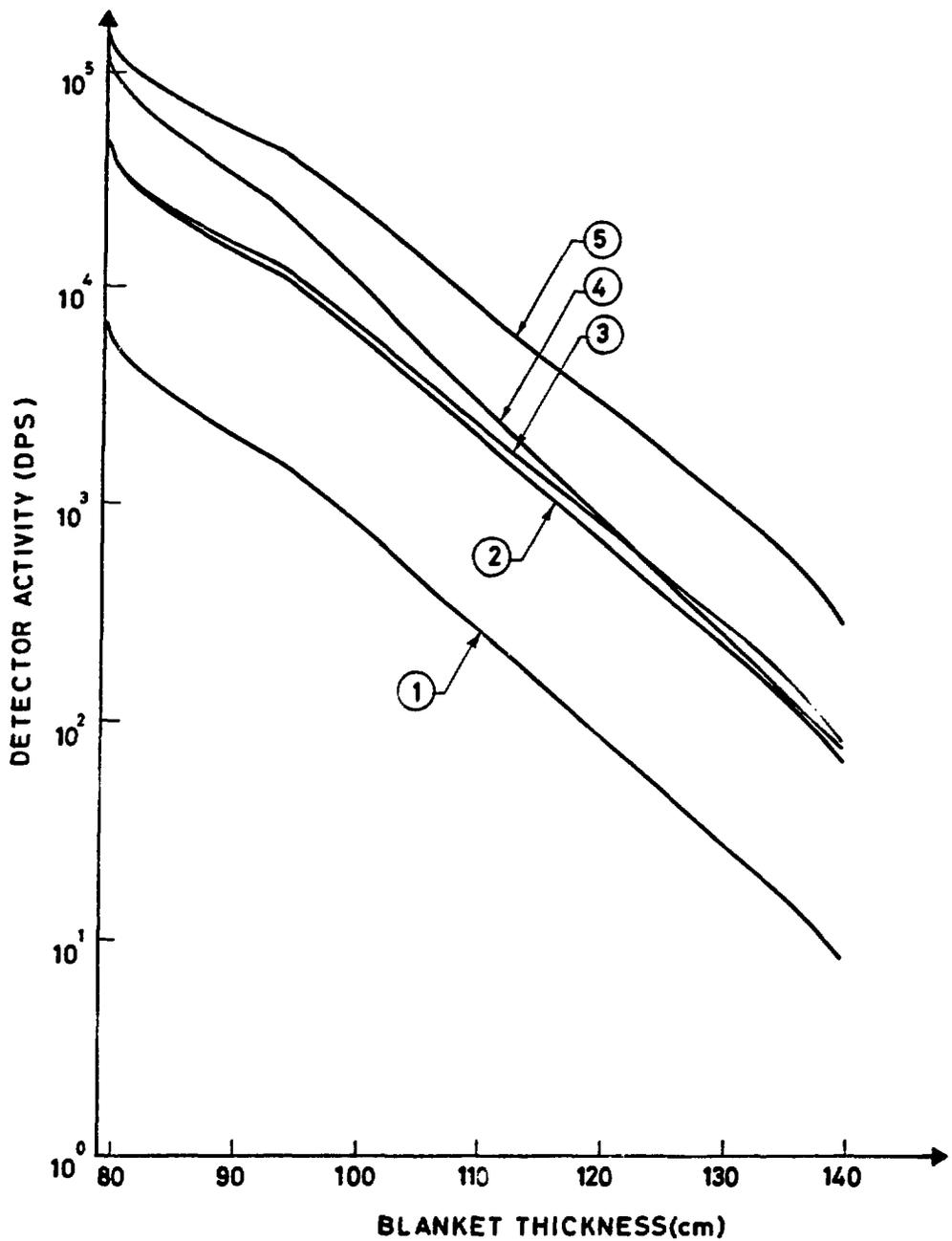
Figure 7. Pertinent threshold detector responses in the blanket for an irradiation time of 8 hours.

1) Cu (n,p)

2) Fe (n,p)

3) Th^{232}(n,f)

4) Cu (n,2n)

5) U^{238}(n,f)
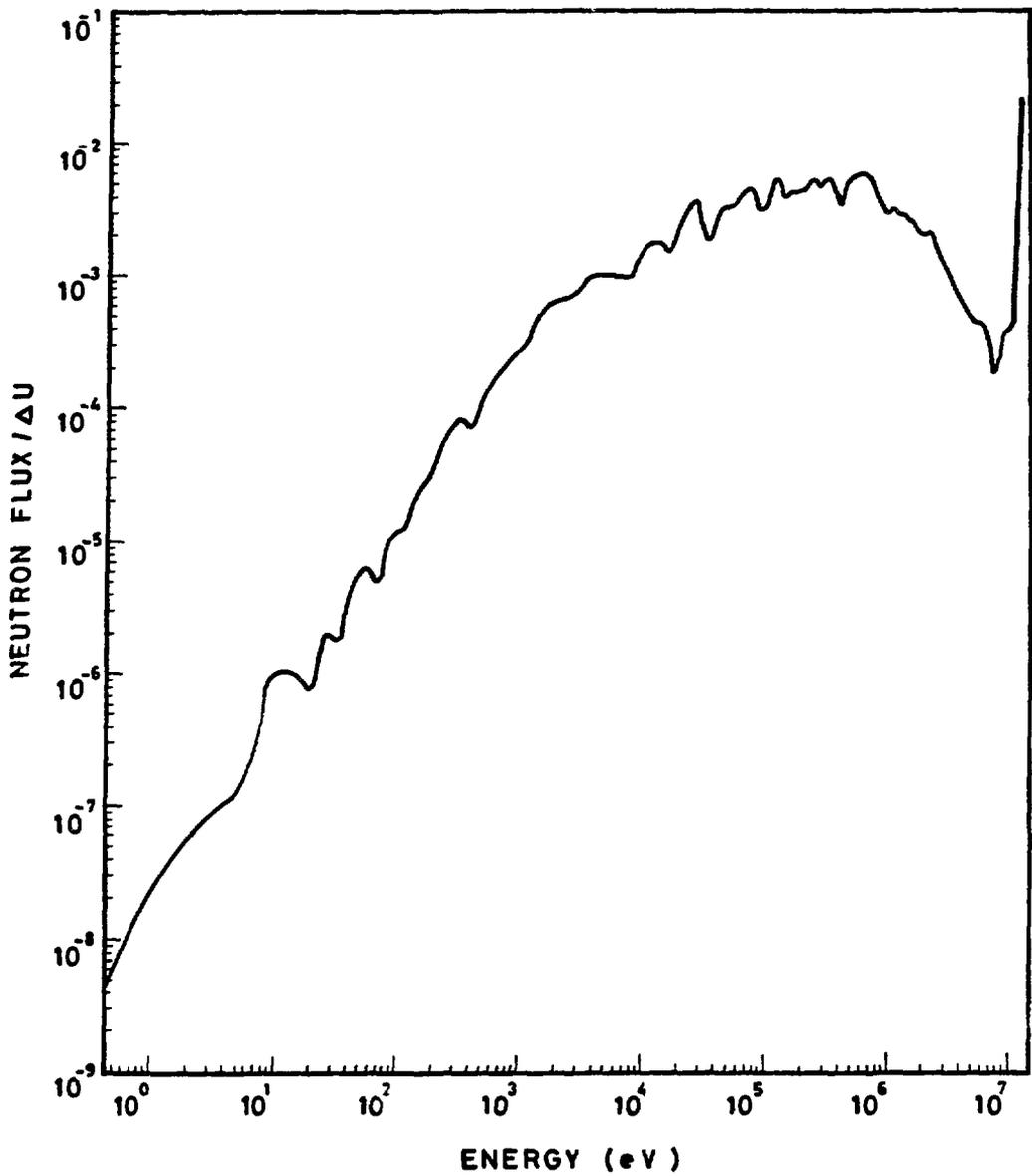
Figure 8. Neutron spectrum in the first wall of the blanket D.
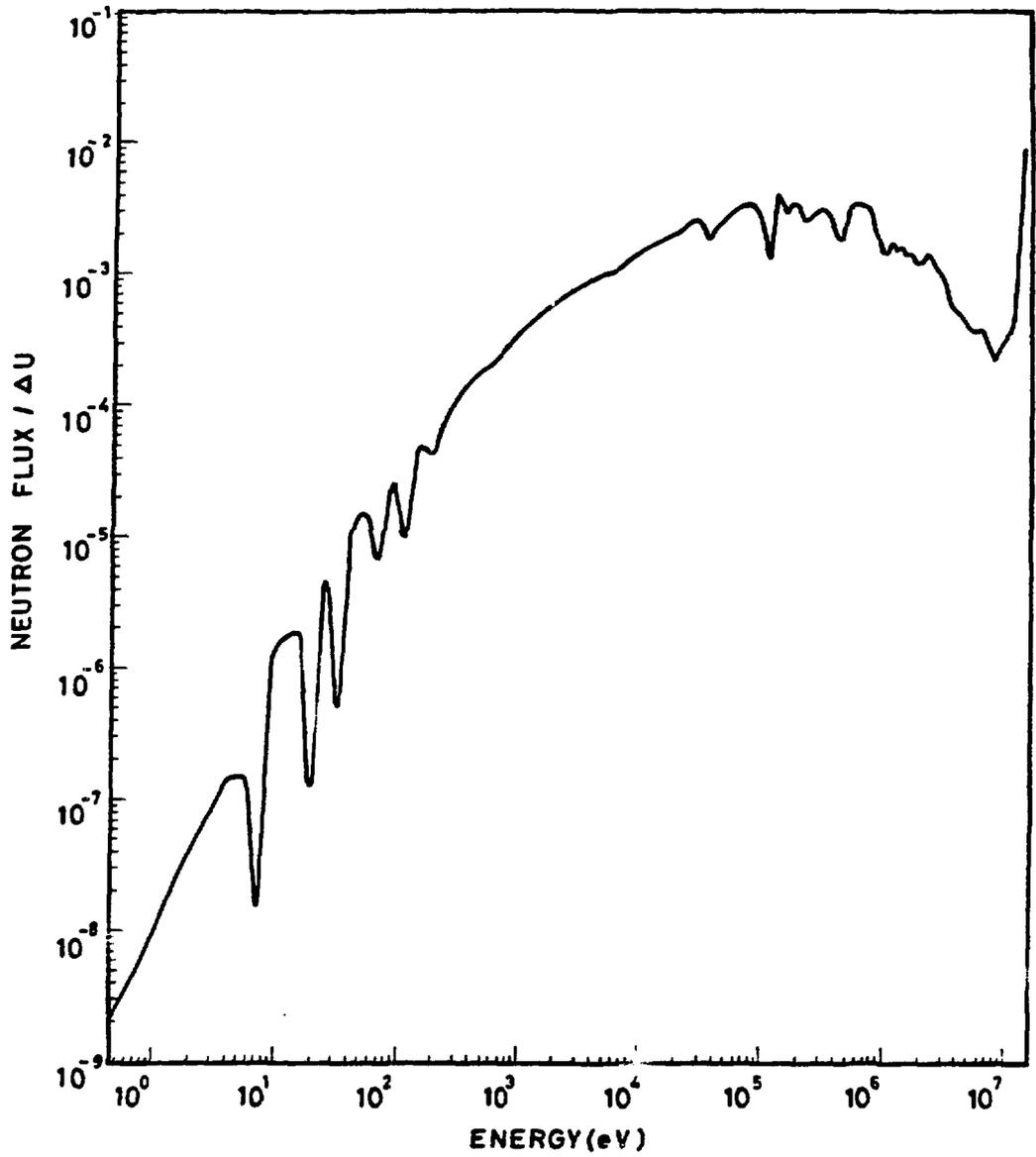
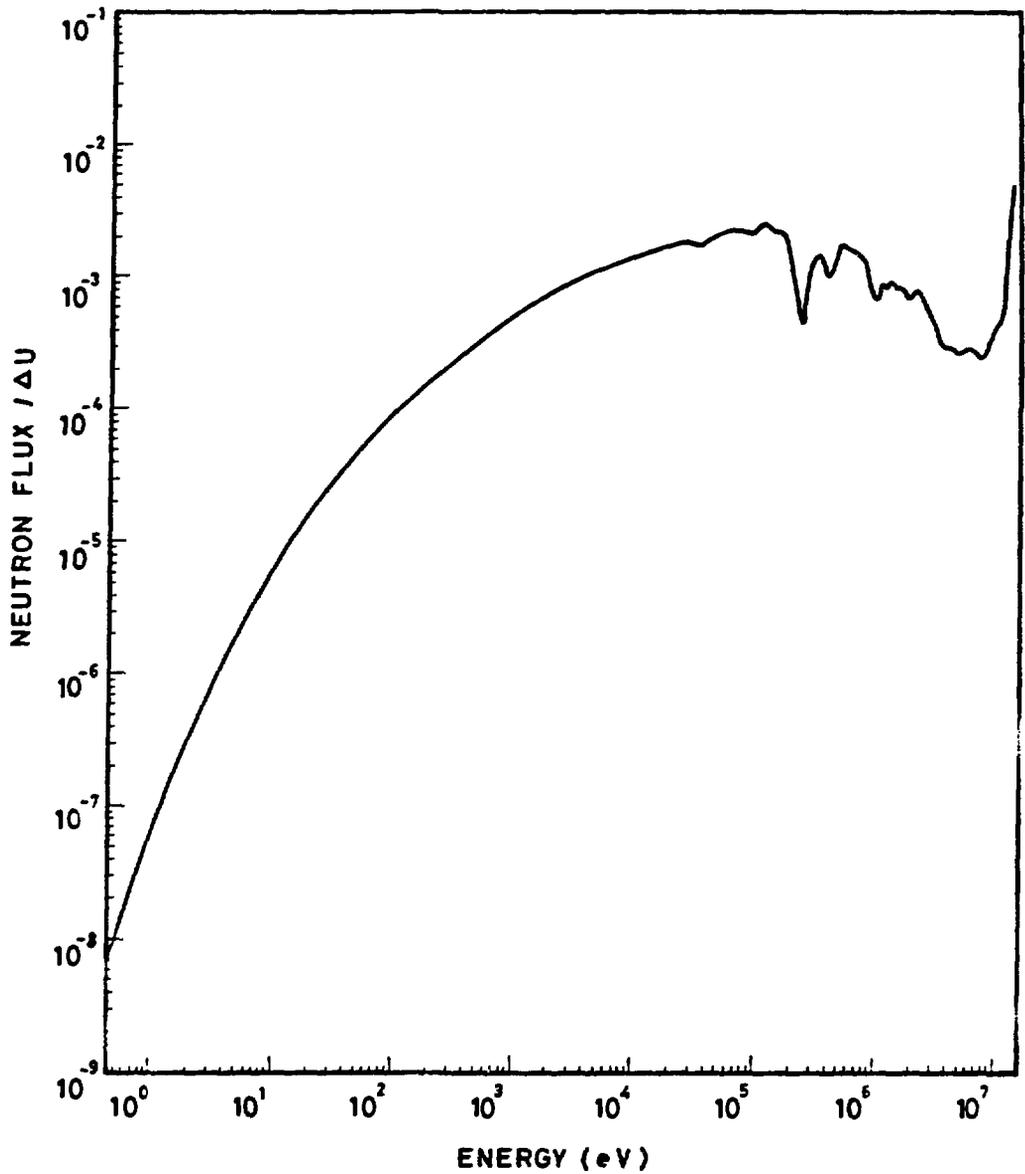Figure 9. Neutron spectrum in the center of the fuel zone.

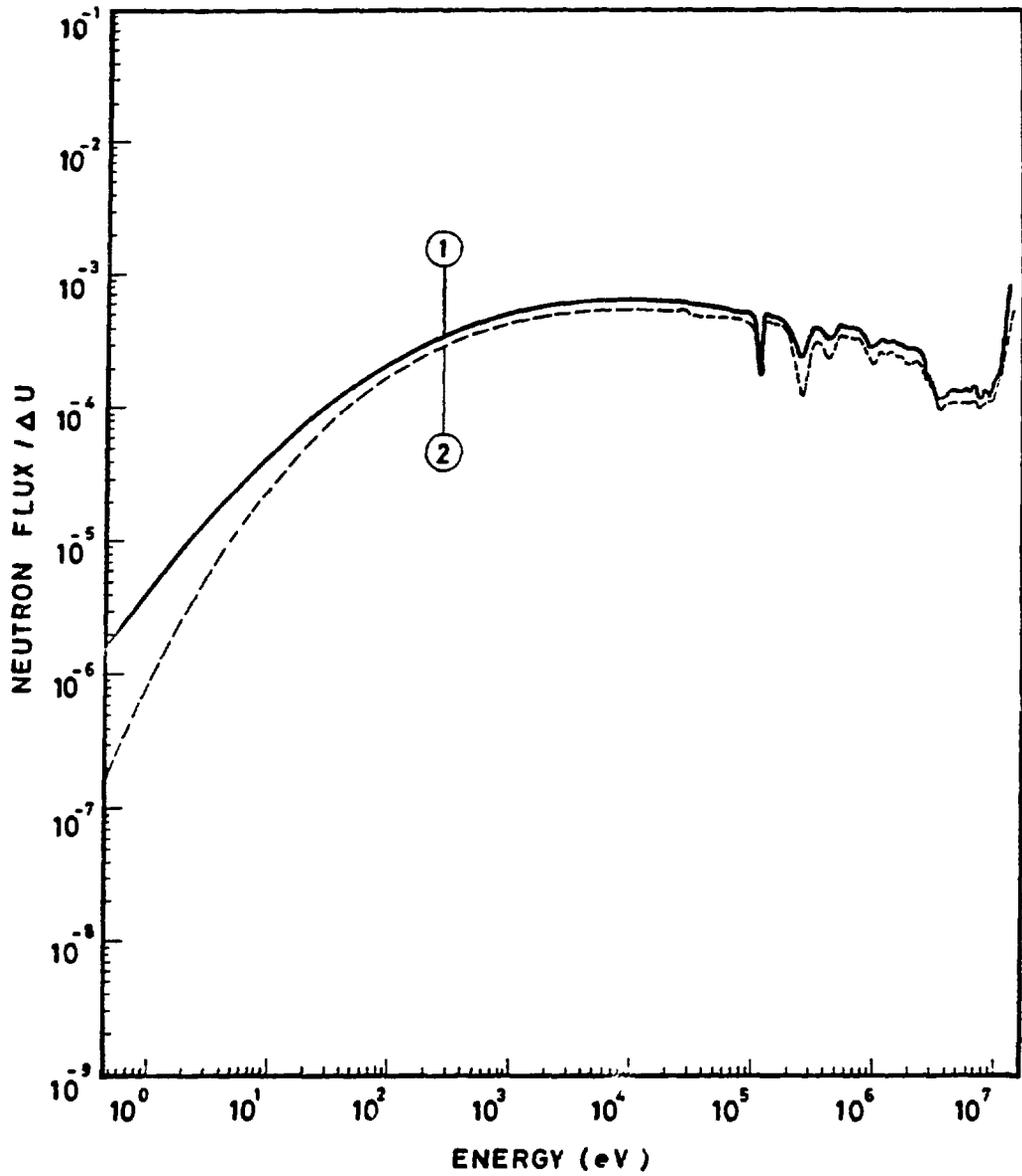Figure 10. Neutron spectrum in the first Li_2O zone adjacent to the fuel zone.

Figure 11. Neutron spectrum in the second Li$_2$O zone
1) Adjacent to the internal graphite zone
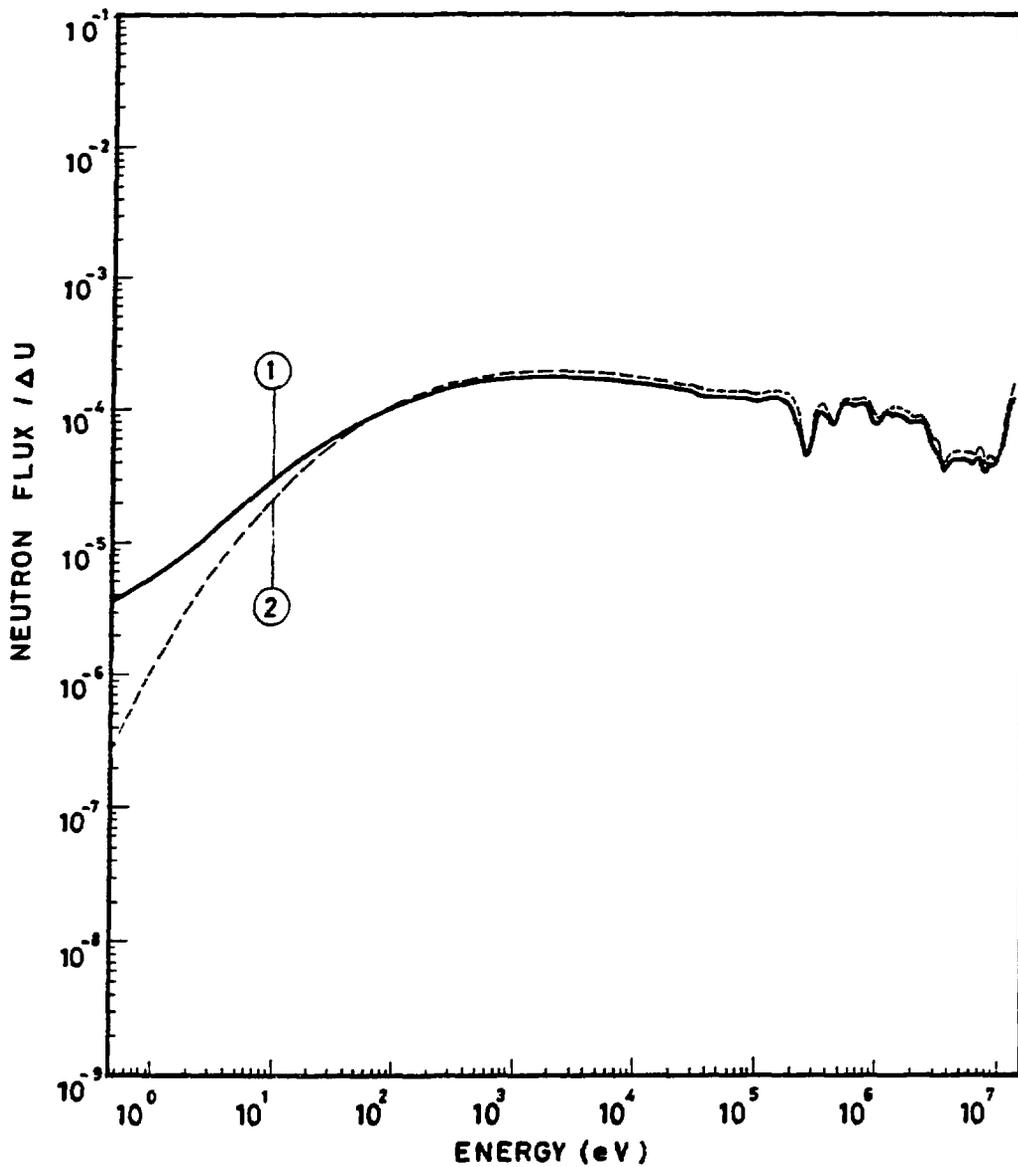2) In the center of Li$_2$O zone.

Figure 12. Neutron spectrum in the third Li_2O zone

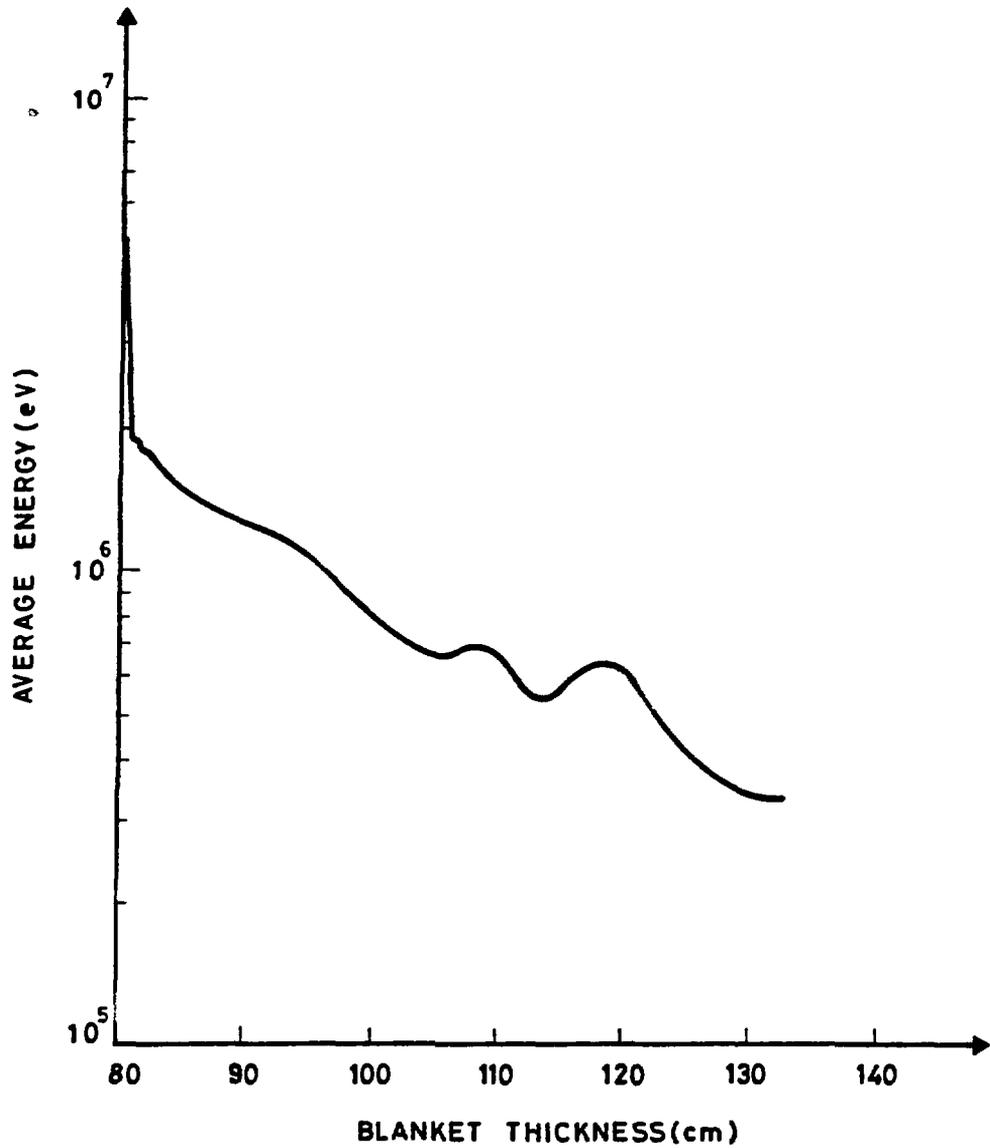   1) Adjacent to the internal graphite zone
        2) In the center of Li_2O zone.

Figure 13. Average neutron energy in the blanket.